

Hypercapnic normalization of BOLD fMRI: comparison across field strengths and pulse sequences

Eric R. Cohen,^{a,b} Egill Rostrup,^c Karam Sidaros,^c Torben E. Lund,^c Olaf B. Paulson,^c Kamil Ugurbil,^a and Seong-Gi Kim^{a,d,*}

^aCenter for Magnetic Resonance Research, University of Minnesota, Minneapolis, MN 15260, United States

^bNeuroscience Program, State University of New York Upstate Medical University, Syracuse, NY 13210-2375, United States

^cDanish Research Centre for Magnetic Resonance, Copenhagen University Hospital, Hvidovre, DK, Denmark

^dDepartment of Neurobiology, University of Pittsburgh, Pittsburgh, PA 55455-0436, United States

Received 14 February 2004; revised 29 April 2004; accepted 18 June 2004
Available online 12 September 2004

The blood oxygenation level-dependent (BOLD) functional magnetic resonance imaging (fMRI) signal response to neural stimulation is influenced by many factors that are unrelated to the stimulus. These factors are physiological, such as the resting venous cerebral blood volume (CBV_v) and vessel size, as well as experimental, such as pulse sequence and static magnetic field strength (B₀). Thus, it is difficult to compare task-induced fMRI signals across subjects, field strengths, and pulse sequences. This problem can be overcome by normalizing the neural activity-induced BOLD fMRI response by a global hypercapnia-induced BOLD signal. To demonstrate the effectiveness of the BOLD normalization approach, gradient-echo BOLD fMRI at 1.5, 4, and 7 T and spin-echo BOLD fMRI at 4 T were performed in human subjects. For neural stimulation, subjects performed sequential finger movements at 2 Hz, while for global stimulation, subjects breathed a 5% CO₂ gas mixture. Under all conditions, voxels containing primarily large veins and those containing primarily active tissue (i.e., capillaries and small veins) showed distinguishable behavior after hypercapnic normalization. This allowed functional activity to be more accurately localized and quantified based on changes in venous blood oxygenation alone. The normalized BOLD signal induced by the motor task was consistent across different magnetic fields and pulse sequences, and corresponded well with cerebral blood flow measurements. Our data suggest that the hypercapnic normalization approach can improve the spatial specificity and interpretation of BOLD signals, allowing comparison of BOLD signals across subjects, field strengths, and pulse sequences. A theoretical framework for this method is provided.

© 2004 Elsevier Inc. All rights reserved.

Keywords: fMRI; High magnetic fields; Brain mapping; Hypercapnia

Introduction

As a simple, indirect indicator of neural activity, the blood oxygenation level-dependent (BOLD) functional magnetic resonance imaging (fMRI) response works remarkably well. It is robust, noninvasive, and spatially and temporally resolved. However, as a precise quantitative index or spatial marker for neural activation, the conventional BOLD response is problematic. The interpretation of the relative change in BOLD signal is complicated by the fact that it depends on the resting capillary and venous cerebral blood volume (CBV_v), in addition to vessel size and orientation, static magnetic field strength (B₀), and pulse sequence (Boxerman et al., 1995b; Frahm et al., 1994; Ogawa et al., 1993). Such factors add complexity to the already intricate relationship between changes in the hemodynamic and metabolic variables that comprise the BOLD response and between these variables and the underlying neuronal activity. Consequently, a fractional change in the BOLD signal does not translate directly into an equivalent fractional change in neural activity. Furthermore, the baseline CBV_v dependence of the BOLD response to a neural stimulus or task implies that active voxels are weighted by vessel size. Large vessels typically show large BOLD changes, depending on pulse sequence and B₀, despite being distant from the actual sites of activity (e.g., Menon et al., 1993; Ogawa et al., 1993; Turner, 2002). Therefore, the distribution of task-induced changes in a typical BOLD activation map does not necessarily reflect the true distribution of brain activity. Both of these issues—the paucity in our ability to quantitatively interpret and precisely locate functional activity using BOLD fMRI—impede our ability to compare data across subjects, field strengths, and pulse sequences (see review by Ogawa et al., 1998).

Several methods have previously been described to reduce macrovascular BOLD signals. These include the use of spin-echo pulse sequences (Bandettini et al., 1994; Boxerman et al., 1995b; Duong et al., 2003; Kennan et al., 1994; Lee et al., 1999; Ogawa et al., 1993; Yacoub et al., 2003), application of diffusion gradients

* Corresponding author. Brain Imaging Research Center, 3025 East Carson Street, Pittsburgh, PA 15237. Fax: +1 412 383 6799.

E-mail address: kimg@pitt.edu (S.-G. Kim).

Available online on ScienceDirect (www.sciencedirect.com.)

(Boxerman et al., 1995a; Lee et al., 1999; Song et al., 1996), and injection of intravascular contrast agents (Rosen et al., 1991). While these methods demonstrate some ability to reduce signals from large veins, each has its limitations. Spin-echo imaging can partially reduce the extravascular signal associated with large veins but is ineffective in reducing the intravascular portion, especially at low magnetic field, leaving a large residual macrovascular blood signal (Oja et al., 1999). SE fMRI, therefore, only has value at high fields (Duong et al., 2003; Lee et al., 1999; Yacoub et al., 2003) that are not in widespread use for human functional imaging. Conversely, diffusion gradients can reduce the intravascular but not the extravascular signal of large veins. However, this technique, too, may suffer from a substantial residual large-vessel signal at low field (Song et al., 1996, 2002), although less so at high field (Lee et al., 1999), and may also partially suppress the desired tissue signal. Injection of intravascular contrast agent may enhance microvascular signals relative to macrovascular signals (Rosen et al., 1991), but this approach detracts from fMRI's appeal as a noninvasiveness mapping technique. Importantly, none of these methods removes the other intrinsic dependencies of the BOLD response, such as those related to field strength and vascular geometry, and therefore they do not allow for quantitative comparisons of BOLD data across experimental settings and subjects. Field-independent changes in perfusion (Edelman et al., 1994; Kim, 1995; Kwong et al., 1992) and oxygen consumption (Davis et al., 1998; Hoge et al., 1999; Hyder et al., 2001; Kim and Ugurbil, 1997; Kim et al., 1999) can be measured. However, these techniques have poor temporal resolution and signal-to-noise ratios compared to the conventional BOLD technique. Thus, a single method that simultaneously retains the robustness and ease of implementation of BOLD fMRI, eliminates the physiological baseline dependence, particularly signals emanating from large veins, and removes the dependence on experimental factors would be ideal.

If the CBV_v weighting of the BOLD response could be attenuated or removed, the remaining signal would be more indicative of oxygenation changes. This is advantageous because, in principle, the greatest increases in blood oxygenation will occur at or near sites of heightened neuronal activity where CBF has increased. Veins that serve to drain large regions of tissue with various levels of activity will be enriched by oxygen from heavily supplied active locales but diluted by relatively deoxygenated, less active or inactive areas (Turner, 2002). Capillaries and small veins serving tissue that is entirely metabolically active will be highly oxygenated relative to vessels serving tissue that is less metabolically active. To calibrate the BOLD response induced by neural activity, a hypercapnic normalization method was proposed by Bandettini and Wong (1997). Hypercapnic normalization reduces relative signal changes in large vessel areas, which can improve the spatial specificity of the BOLD signal.

In this study, we expanded upon the hypercapnic normalization procedure and compared activation data obtained with gradient echo fMRI at three magnetic fields, 1.5, 4.0, and 7.0 T. We also compared activation data obtained using both gradient echo and spin echo pulse sequences at 4.0 T. Under all conditions, voxels containing primarily large vessels and those containing primarily active tissue (i.e., capillaries and small veins) had distinguishable behavior when normalized by a hypercapnia activation map. These characteristics allowed active tissue to be more specifically localized and allowed activity to be quantified based on changes in blood oxygenation alone. The ratio of the BOLD signal induced

by neural activity to that induced by hypercapnia was consistent across different magnetic fields and pulse sequences, allowing comparison of the normalized BOLD signal across these different experimental conditions.

Theory

BOLD contrast in proton-based magnetic resonance images is determined by the amount of deoxyhemoglobin in red blood cells of capillaries and veins, which causes a susceptibility difference across the blood vessel wall. Because the hemoglobin of arteries and arterioles is approximately 97% saturated with oxygen, there is no susceptibility difference across the walls of these vessels and no associated BOLD contrast relative to the surrounding tissue. The paramagnetism of deoxyhemoglobin affects the bulk magnetic susceptibility of the water in the venous intravascular space and the extravascular space in different manners. The total BOLD signal at echo time TE, $S_{\text{total}}(\text{TE})$, will be given by the volume-weighted sum of the intravascular and extravascular signals as

$$S_{\text{total}}(\text{TE}) = (1 - f) \times S_{\text{ev}}^0 \times \exp(-\text{TE} \times R_{2\text{ev}}^*) + f \times S_{\text{iv}}^0 \exp(-\text{TE} \times R_{2\text{iv}}^*), \quad (1)$$

where S_{ev}^0 and S_{iv}^0 are the intrinsic signals at TE = 0 in the extravascular and intravascular compartments, respectively, f is the venous intravascular fractional blood volume contribution to the total intravoxel volume, and $R_{2\text{ev}}^*$ and $R_{2\text{iv}}^*$ are the apparent transverse relaxation rates of the extravascular and intravascular compartments, respectively. We assumed that during stimulation, the venous intravascular blood volume fraction does not change, and only changes in $R_{2\text{ev}}^*$ and $R_{2\text{iv}}^*$ exist. Note that although the arteriolar CBV can change considerably in response to neural stimulation (Ngai et al., 1995), nearly complete oxygen saturation of hemoglobin in these vessels, as mentioned above, causes the arteriolar susceptibility to be similar to that of the surrounding tissue. Hence, changes in the balance of arteriolar intravascular and extravascular fractional blood volume are inconsequential with respect to BOLD contrast. Defining the venous extravascular and intravascular apparent transverse relaxation rates during the control condition as $R_{2\text{ev}}^*(\text{cont})$ and $R_{2\text{iv}}^*(\text{cont})$, respectively, and during the stimulus condition as $R_{2\text{ev}}^*(\text{st}) = R_{2\text{ev}}^*(\text{cont}) + \Delta R_{2\text{ev}}^*$ and $R_{2\text{iv}}^*(\text{st}) = R_{2\text{iv}}^*(\text{cont}) + \Delta R_{2\text{iv}}^*$, respectively, the change in the total BOLD signal is

$$\begin{aligned} \Delta S_{\text{total}}(\text{TE}) &= (1 - f) \times [S_{\text{ev}}^0 \times \exp(-\text{TE} \times R_{2\text{ev}}^*(\text{cont})) \\ &\quad \times (\exp(-\text{TE} \times \Delta R_{2\text{ev}}^*) - 1)] + f \\ &\quad \times [S_{\text{iv}}^0 \cdot \exp(-\text{TE} \times R_{2\text{iv}}^*(\text{cont})) \\ &\quad \times (\exp(-\text{TE} \times \Delta R_{2\text{iv}}^*) - 1)]. \end{aligned} \quad (2)$$

After a linear approximation of the exponentials containing $\Delta R_{2\text{ev}}^*$ and $\Delta R_{2\text{iv}}^*$, Eq. (2) can be simplified to

$$\Delta S_{\text{total}}(\text{TE}) \approx -k_{\text{ev}} \times \text{TE} \times \Delta R_{2\text{ev}}^* - k_{\text{iv}} \times \text{TE} \times \Delta R_{2\text{iv}}^* \quad (3)$$

where $k_{\text{ev}} = (1 - f) \times S_{\text{ev}}^0 \times \exp(-\text{TE} \times R_{2\text{ev}}^*(\text{cont}))$ and $k_{\text{iv}} = f \times S_{\text{iv}}^0 \times \exp(-\text{TE} \times R_{2\text{iv}}^*(\text{cont}))$ are constants.

The effective transverse relaxation rate of the extravascular water induced by deoxyhemoglobin in blood can be expressed as

$$R_{2ev}^* = 1/T_{2ev}^* = \alpha \times CBV_v \times (1 - Y)^\beta, \quad (4)$$

where α and β are constants, Y is the venous hemoglobin saturation in the baseline or control state, and CBV_v is the capillary and venous cerebral blood volume that contributes to the BOLD signal (Kim et al., 1999; Ogawa et al., 1993). The constant α depends on several factors, including magnetic field strength, vessel size and orientation, hematocrit, and the susceptibility difference between completely oxygenated and completely deoxygenated blood. It can therefore vary with subject and brain region. The exponent β depends on vessel size and magnetic field strength. It has been shown that R_{2ev}^* around microvessels (i.e., vessels with a radius less than 8 μm) depends quadratically on field strength whereas that associated with large vessels depends linearly on field strength (Ogawa et al., 1993; Boxerman et al., 1995b). Because any given image voxel will contain a mixture of large and small vessels, the value of β will vary between 1.0 and 2.0 according to the vascular milieu of the voxel and will shift toward a quadratic dependence, in favor of small blood vessels, at high magnetic field strength (Ogawa et al., 1993).

A stimulus will induce a change in R_{2ev}^* by modulating venous oxygenation level and venous blood volume. The change in venous blood volume (CBV_v) that contributes to the BOLD signal has been measured in rats (Lee et al., 2001). It was demonstrated that $\Delta CBV_v / CBV_v = 0.15 \times \Delta CBF / CBF$, where $\Delta CBF / CBF$ is the relative change in CBF that accompanies a moderate hypercapnic stimulus. This venous blood volume change is considerably smaller than the total change in CBV, $\Delta CBV / CBV = 0.31 \times \Delta CBF / CBF$ (Grubb et al., 1974; Haacke et al., 1997; Lee et al., 2001). A complex motor task-induced change in CBF can be about 25–30% (Kim, 1995; Kim and Tsekos, 1997; Zaini et al., 1999). Therefore, under these circumstances, the relative change in CBV that contributes to the BOLD signal would be approximately $(0.15)(0.3) = 0.045$ or 4.5%. The typical activation-induced changes in venous oxygenation can be approximately 30% (e.g., from $Y = 0.54$ to 0.68; Haacke et al., 1997). Because ΔY is substantially greater than the change in CBV_v and is therefore the dominant factor in determining the magnitude of the BOLD response, the change

in CBV_v was ignored in deriving an expression for ΔR_{2ev}^* . By keeping only the first-order changes in ΔY , the change in R_{2ev}^* can be described by

$$\begin{aligned} \Delta R_{2ev}^* &\approx \alpha \times CBV_v \times (1 - Y)^\beta \{ -\beta \Delta Y / (1 - Y) \} \\ &= \alpha^* \times \Delta Y, \end{aligned}$$

where $\alpha^* = -\alpha \times \beta \times CBV_v (1 - Y)^{\beta-1}$ is a constant. Note that the change in the extravascular transverse relaxation rate depends on the resting CBV_v .

Based on the Luz–Meiboom model applied by Wright et al. (1991), the transverse relaxation rate of blood can be described as

$$R_{2iv}^* = 1/T_{2iv}^* = 1/T_2^o + C(1 - Y)^2, \quad (6)$$

where $1/T_2^o$ is the transverse relaxation rate of fully oxygenated blood and C is a constant that depends quadratically on field strength and linearly on hematocrit. The stimulus-induced change in R_{2iv}^* can be expressed by the difference equation

$$\Delta R_{2iv}^* = 1/T_2^o + C(1 - Y - \Delta Y)^2 - (1/T_2^o + C(1 - Y)^2).$$

This can be simplified to

$$\Delta R_{2iv}^* = C[-2 \times \Delta Y(1 - Y) + \Delta Y^2].$$

Finally, keeping only first-order terms, the stimulus-induced change in R_{2iv}^* can be expressed as

$$\Delta R_{2iv}^* \approx -2C \times \Delta Y(1 - Y) = C^* \times \Delta Y, \quad (7)$$

where $C^* = -2C \times (1 - Y)$ is a constant. When Eqs. (5) and (7) are inserted into Eq. (3), Eq. (3) can be rewritten succinctly as

$$\begin{aligned} DS_{\text{total}}(TE) &\approx -k_{ev}^* \times TE \times \Delta Y - k_{iv}^* \times TE \times \Delta Y \\ &= k_{\text{total}} \times TE \times \Delta Y, \end{aligned} \quad (8)$$

where $k_{ev}^* = k_{ev} \times \alpha^*$, $k_{iv}^* = k_{iv} \times C^*$, and $k_{\text{total}} = -k_{ev}^* - k_{iv}^*$. Thus, the change in the BOLD signal is proportional to the change

Table 1

Intersubject average values of ΔR_{2ev}^* and ΔR_2 for the finger movement task and for the hypercapnic challenge, normalized change in the BOLD signal ($\Delta BOLD_{\text{norm}}$), and relative change in CBF (rCBF) at each field strength and pulse sequence ($n = 5, 8,$ and 3 for the GE studies at 1.5, 4, and 7 T, respectively, and $n = 6$ for the SE study at 4 T)

B_0 (T)	Pulse sequence	BOLD			CBF		
		Number of pixels	Motor ΔR_{2ev}^* or ΔR_2 (s^{-1})	Hypercapnia ΔR_{2ev}^* or ΔR_2 (s^{-1})	Motor $\Delta BOLD_{\text{norm}}$	Motor rCBF (%)	Number of pixels
1.5	GE	180 (69)	0.21 ^a (0.06)	0.36 ^c (0.26)	0.75 (0.37)	24.2 (5.5)	137 (66)
4	GE	203 (86)	0.69 ^{a,b} (0.26)	1.42 ^{c,d} (0.71)	0.59 (0.36)	23.8 (7.8)	151 (42)
4	SE	144 (46)	0.24 ^b (0.05)	0.36 ^d (0.10)	0.71 (0.24)	26.3 (4.9)	129 (40)
7	GE	184 (52)	0.91 ^a (0.08)	1.62 ^c (0.30)	0.57 (0.07)	29.4 (12.1)	150 (37)

The average number of pixels within the ROI for each parameter is given. One standard deviation of the mean is given in parentheses. Mean activation levels were tested for statistically significant differences, as noted in the text. Significant differences were found between groups of subjects for GE motor and hypercapnia ΔR_{2ev}^* (^a $P < 0.001$ and ^c $P < 0.01$, respectively). Differences between the 4-T SE and GE motor ΔR_{2ev}^* values and between 4-T SE and GE hypercapnia ΔR_{2ev}^* values were also found to be significant (^b $P < 0.005$ and ^d $P < 0.01$, respectively). No significant differences were found between groups with respect to motor $\Delta BOLD_{\text{norm}}$ and motor rCBF.

in venous oxygenation, which is closely related to metabolic activity. Note, however, that both k_{ev}^* and k_{iv}^* , and hence k_{total} , are linearly related to resting CBV_v , which is unrelated to metabolic activity. The constant k_{ev}^* includes α^* , which is directly proportional to CBV_v . The constant k_{iv}^* is proportional to f , the fractional CBV of the voxel. Additionally, because the constant k_{total} is dependent on many factors including vascular structure, magnetic field strength, and data acquisition methods, it is difficult to compare data for a given stimulus or task across subjects and field strengths quantitatively.

In a typical fMRI study, a stimulus-induced BOLD signal change divided by a baseline BOLD signal (rBOLD) is used to indicate the strength of underlying activity. The relative change in the BOLD signal rBOLD can be described as

$$\begin{aligned} \text{rBOLD} &= \Delta S_{total}(TE) / S_{total}(TE) \\ &= k_{total} \times TE \times \Delta Y / S_{total}(TE) \approx -\Delta R_2^* \times TE, \end{aligned} \quad (9)$$

where ΔR_2^* is the change in the apparent transverse relaxation rate induced by stimulation. The approximation $\text{rBOLD} \approx -\Delta R_2^* \times TE$ is valid when $-\Delta R_2^* \times TE \ll 1$, which is the case for a typical fMRI study. TE is usually set to $1/R_2^*$ to maximize the BOLD signal change. Note that the optimal TE varies with field strength and pulse sequence (Ogawa et al., 1993), hindering the task of comparing rBOLD measured under different conditions. To facilitate comparison of data obtained using different, optimal TE's, the effect of TE can be eliminated by using ΔR_2^* in place of rBOLD. Because $S_{total}(TE)$ can be normalized to 1.0, $\Delta R_2^* = -k_{total} \times \Delta Y = -\text{rBOLD}/TE$.

To remove the constant k_{total} contribution from fMRI data, a normalization experiment can be performed, generating the same k_{total} as the neural stimulus and a ΔY that is homogenous across pixels from a cortical region. This can be accomplished by inducing moderate hypercapnia, which has the effect of elevating the CBF and BOLD signals without increasing metabolic activity (Kety and Schmidt, 1948). Normalizing the neural stimulus-induced change $\Delta S_{total(st)}$ by the hypercapnia-induced change $\Delta S_{total(hc)}$, the normalized signal change or ratio $\Delta \text{BOLD}_{norm}$ is obtained:

$$\begin{aligned} \Delta \text{BOLD}_{norm} &= \Delta S_{total(st)} / \Delta S_{total(hc)} \\ &= \text{rBOLD}_{(st)} / \text{rBOLD}_{(hc)} = \Delta Y_{st} / \Delta Y_{hc}. \end{aligned} \quad (10)$$

Because the increase in CBF that occurs during hypercapnia is uniform for at least a given region of the brain (Ito et al., 2000), the change in venous oxygenation during hypercapnia should also be constant across pixels from a given region of cortex. Therefore, the normalized ratio $\Delta \text{BOLD}_{norm}$ reflects the change in venous oxygenation during stimulation scaled by the constant change in capillary and venous oxygenation during hypercapnia and does not depend on resting CBV_v . Inasmuch as a change in vascular oxygenation is associated with metabolic activity and baseline CBV_v is not, the map of normalized signal change indicates sites of true activation rather than emphasizing areas of large resting blood volume. Furthermore, there is no dependence on any other factors such as field strength, vascular geometry, or pulse sequence, allowing comparison of data across multiple experimental conditions and subjects in a quantitative manner.

Methods

Subjects

Subjects for these studies were in good health and gave informed consent to participate in accordance with the guidelines of the local ethics committees. Some subjects participated more than once. Data were analyzed from a total of 18 subjects: 5 at 1.5 T (mean age 24.2 ± 2.9 , all female), 10 at 4 T (mean age 28.1 ± 7.0 , five female, five male), and 3 at 7 T (mean age 25.0 ± 2.6 , two female, one male). Data from other participants were discarded due to excessive head motion or technical artifacts.

Imaging

Experiments were conducted at three magnetic field strengths, 1.5 T (Siemens Vision), 4 T (Siemens), and 7 T (Magnex Scientific Ltd.). The 1.5-T experiments were run from a clinical console and used a Siemens transmit–receive head coil. The 4- and 7-T magnets were driven by Varian Unity^{INNOVA} consoles (Varian, Inc., Palo Alto, CA) and used home-built head coils with a TEM design for RF transmission and reception (Vaughan et al., 1994). Anatomical images were acquired with a 2D, inversion-prepared fast low-angle shot (TurboFLASH) imaging sequence (TR = 0.011 s, TE = 5 ms, TI = 1.4 s, flip angle = 20° , matrix size = 128×128 , field of view = $21 \times 21 \text{ cm}^2$, slice thickness = 5 mm). At all field strengths, functional images were obtained with a gradient echo (GE) echo-planar imaging (EPI) pulse sequence on a single slice with matrix size = 64×64 , field of view = $21 \times 21 \text{ cm}^2$, and slice thickness = 5 mm. T₂^{*}-weighted BOLD images (TE = 50, 30, and 25 ms at 1.5, 4, and 7 T, respectively, flip angle = 60°) were interleaved between the slice-selective and non-slice-selective inversion recovery (IR) images of a flow alternating inversion recovery (FAIR) pulse sequence (TE = 22 ms, 16 ms, and 18 ms at 1.5 T, 4 T, and 7 T, respectively, TI = 1.4 s) (Kim, 1995). A repetition time (TR) of 1.6 s followed each BOLD and IR excitation pulse resulting in an effective temporal resolution of 9.2 s for the experiment. The centers of the echo trains were shifted within the acquisition window to achieve a single-shot echo-planar image with a maximal contrast-to-noise ratio. Additional experiments at 4 T were carried out with a spin echo (SE) EPI sequence in which the flip angle = 90° and the TE = 44 ms for both BOLD and FAIR images, but all other parameters and details of the experiment were the same as those of the GE experiments.

Experiment protocol

Each subject lay supine inside the magnet bore with his or her head situated in the head coil. The sides of the head were packed with foam cushions to minimize head motion. The subject's pulse and respiration waveforms were continuously monitored with a pulse oximeter and a respiration belt and, at 4 and 7 T, recorded by a desktop computer running Acknowledge software (Biopac Systems, Inc., Santa Barbara, CA). At the beginning of the study, axial and sagittal scout images were obtained to assess proper head position, following which shimming was performed over the entire head. Several axial anatomic images were then obtained to find the precentral gyrus, which contains the primary motor cortex (M1). In some subjects, a functional BOLD localizer experiment was performed to best identify the slice that contained the hand area of M1. Based on the sulcal anatomy and the functional localizer

experiment, a single axial slice was chosen for the remainder of the study.

Each scanning session included a hypercapnia experiment using a 5% CO₂ (21% O₂, 74% N₂) gas mixture and one or more runs of sequential finger movements. The method for inducing hypercapnia in the current study was the same as that used by Cohen et al. (2002) and similar to that used by Rostrup et al. (1994). In both studies, hypercapnia was induced with 5% CO₂ inhalation. Before participating in the experiment, subjects were given the opportunity to breathe the normal and 5% CO₂ gas mixture for several minutes outside of the magnet. This was done to determine whether any adverse or uncomfortable effects were experienced, if the subject had any difficulties breathing through a tube, if the subject had difficulty tolerating hypercapnia for an extended period, and to find a comfortable gas flow rate for each volunteer.

The hypercapnia fMRI experiment consisted of 360 individual images collected by the interleaved BOLD/FAIR sequence to generate 90 average BOLD images and 90 perfusion images. This experiment lasted approximately 13.5 min during which two 3-min epochs of hypercapnia were induced. During these runs, the subject's nose was closed with a nose clip and the subject breathed through a plastic mouthpiece. Air was delivered at approximately 15–25 l/min through corrugated tubing attached to the mouthpiece. The air was filtered and humidified with a heat moisture exchanger (Baxter Healthcare Corp., Deerfield, IL) placed in line with the tubing. During the hypercapnia experiments, the experimenter initiated the 3-min elevation of inspired CO₂ by switching the gas manually with a three-way valve from normal air to CO₂-enriched air.

The sequential finger movement exercise was performed at a rate of 2 Hz, paced by red LED goggles (at 4 and 7 T) or an auditory cue (at 1.5 T). The experiment consisted of 200 images collected by the interleaved BOLD/FAIR sequence to generate 50 averaged BOLD images and 50 perfusion images. The experiment lasted 7.5 min during which two 1.5-min epochs of finger movements were performed. The exercise was performed by having the subject oppose the thumb and each of the other digits, starting first with the index finger, progressing to the little finger, repeating the little finger, and progressing back to the index finger. This sequence was repeated throughout the movement epoch.

Image postprocessing and data analysis

All functional images were Gaussian filtered in k-space and zero-filled to a 128 × 128 matrix size. FAIR difference images were obtained by subtracting each non-slice-selective IR image from the subsequent slice-selective IR image. Images were realigned using SPM99 (Wellcome Department of Imaging Neuroscience, <http://www.fil.ion.ucl.ac.uk/spm/spm99.html>; Friston et al., 1995). Temporally adjacent BOLD images were averaged so that the BOLD series and FAIR series contained the same number of images.

Generation of activation maps

Activation maps were generated for the hypercapnia and motor task data by calculating a cross-correlation coefficient on a pixel-by-pixel basis from the BOLD image time series ($P \leq 0.05$ for 4-T SE and 1.5-T GE data, $P \leq 0.01$ for 4- and 7-T GE data; P values are uncorrected for multiple comparisons). From statistically active pixels, the relative change in the BOLD signal, $rBOLD = \Delta BOLD/$

$BOLD$, and the negative change in transverse relaxation rate, $-\Delta R_2^* = rBOLD/TE$, were computed. Note that the term $\Delta BOLD$ is identical to $\Delta S_{total}(TE)$ in Eq. (8) and is used throughout the remainder of the article; the terminology has been changed to make a clear distinction between the BOLD and CBF signals. Furthermore, to simplify the notation, $-\Delta R_2^*$ will be referred to in the text and figures as ΔR_2^* .

Activation maps based on percent change in CBF (rCBF) were created from the FAIR data from the same statistically active pixels used in creating the rBOLD and ΔR_2^* maps. To correct for BOLD contributions to the CBF signal, the formula $rCBF = (rFAIR + 1)/(rBOLD(TE_{FAIR}/TE_{BOLD}) + 1) - 1$ was used, where $rFAIR = \Delta FAIR/FAIR$ is the relative change in the FAIR signal. On average, this correction amounted to approximately 5% of the relative FAIR signal change.

Activation maps were mildly low-pass filtered by convolution with a normalized 3 × 3 voxel standard Gaussian kernel (FWHM = 7.72 mm). These statistically thresholded, filtered activation maps were used for all subsequent analyses. To compare signals across magnetic fields and different acquisition methods, a 'motor region ROI' was specified for each subject and included active pixels in the primary sensorimotor and premotor areas in the hemisphere contralateral to the finger movement.

Results

Hypercapnia-induced changes and spatial normalization of the BOLD response

Inhalation of the 5% CO₂ gas mixture resulted in a reliable increase in subjects' end-tidal CO₂ (ETCO₂). The mean ETCO₂ was approximately 48 ± 2.5 mm Hg over all experiments at 4 and 7 T, consistent with our previous studies (Cohen et al., 2002; Rostrup et al., 1994). The mean end-tidal CO₂ during hypercapnia in Cohen et al.'s (2002) study was 46.7 ± 3.2 mm Hg ($n = 5$). In Rostrup et al.'s (1994) study, the PaCO₂ was obtained directly from arterial blood gas measurements and was 46.2 ± 2.6 mm Hg ($n = 6$). For technical reasons, ETCO₂ was not recorded at 1.5 T. None of the subjects described any difficulties breathing 5% CO₂ gas inside the magnet nor reported any uncomfortable sensations such as shortness of breath or anxiety. Fig. 1 shows one representative GE BOLD data set obtained at 4 T. Hypercapnia caused a global BOLD signal increase primarily in the gray matter and to a lesser extent in the white matter (Fig. 1b). The highest signal changes (yellow pixels) were located at the lateral and medial edges of the cortex, territory drained by the large superior cerebral veins that eventually drain into the venous sinuses (Carpenter, 1991; Osborn, 1994). A similar pattern of activation was observed in all measurements, across field strengths, as described in previous studies (Kastrup et al., 2001; Rostrup et al., 1994, 2000). Because hypercapnic stimulation presumably induces a uniform change in venous oxygenation (ΔY) across the cortex, spatial variation in the BOLD signal intensity is due to local variability in resting blood volume and vessel size (Eqs. (5) and (8)). During finger opposition (Fig. 1c), localized activation was observed in the contralateral primary motor and somatosensory cortices and bilaterally in the lateral and medial premotor areas. Similarly, large activation signals were observed in the superior sagittal sinus, interhemispheric fissure, and contralateral cortical edge.

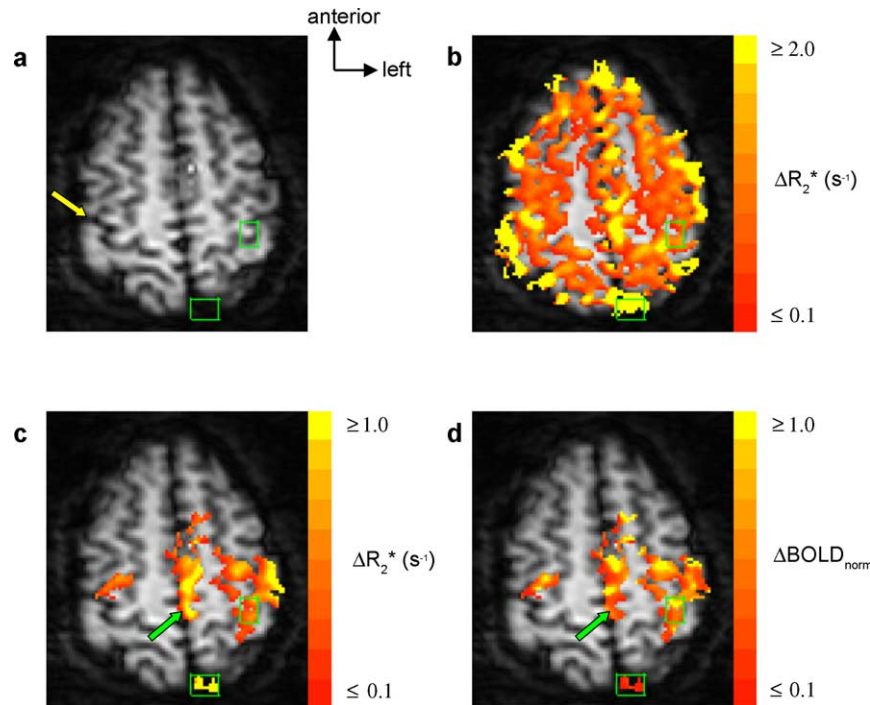


Fig. 1. (a) Average axial GE non-slice-selective IR image from one subject at 4 T. Overlaid on the image are the hypercapnia ΔR_2^* activation map (b), motor ΔR_2^* activation map (c), and hypercapnia normalized motor activation map (d). The yellow arrow in a points to the ipsilateral central sulcus. The color bars correspond to ΔR_2^* in units of s^{-1} in b and c and $\Delta BOLD_{norm}$, which is a unitless ratio, in d. ROIs (green rectangles) were drawn to isolate the superior sagittal sinus and an active region of the sensorimotor cortex, and these points are plotted in Fig. 2 (color). Note the shift in the activation hot spots (yellow) between the motor ΔR_2^* activation map (c) and the normalized motor activation map (d). In particular, the superior sagittal sinus, which was highly active in the motor and hypercapnia ΔR_2^* maps, is only weakly active in the normalized map. Similarly, highly active regions on the edge of the brain near the motor cortex and within the interhemispheric fissure are attenuated in the normalized map. In contrast, activity within the primary sensorimotor cortex is accentuated in the normalized map. Because the normalized map is based on changes in venous oxygenation and is not weighted by blood volume, it is more specific to the sites of actual activity. Note that while sites highly active in the BOLD map, such as the superior sagittal sinus, can be ignored based on known cerebral vascular anatomy, other active sites, such as the one indicated by the green arrow in c, are more ambiguous. This site is apparently very active in the BOLD map but is much less active in the $\Delta BOLD_{norm}$ map (d), indicative of a larger-sized vessel. The normalization procedure is most helpful in these latter situations in which the locations of large veins are not known a priori.

If neural stimulation induced homogeneous oxygenation level changes, one would expect to see a linear relationship between the ΔR_2^* values associated with neural activity and those induced by global stimulation. To evaluate this, ΔR_2^* in the sensorimotor cortex during finger movement was plotted against ΔR_2^* during hypercapnia on a pixel-by-pixel basis (Fig. 2a). A nonlinear, monotonic relationship was observed, consistent with the results of Bandettini and Wong (1997), indicating that the ΔR_2^* associated with a stimulatory task consists of inhomogeneous oxygenation level changes on top of regionally varying resting CBV_v levels.

To remove CBV_v contribution to the BOLD signal, the BOLD response induced by localized neural activity was divided by the response induced by the homogenous global hypercapnic perturbation on a pixel-by-pixel basis, yielding a normalized BOLD change ($\Delta BOLD_{norm}$) map (Fig. 1d). As shown, pixels with high ΔR_2^* do not necessarily coincide with pixels with high $\Delta BOLD_{norm}$ (Figs. 1c and 1d). The most obvious example of this is the superior sagittal sinus, which is highly active in the motor task ΔR_2^* map due to its large resting CBV_v , but only weakly active in the $\Delta BOLD_{norm}$ map due to low changes in oxygenation upon activation. Whereas in the ΔR_2^* motor activation map in which highly active foci could be seen at the edge of the brain, for instance lateral to the left motor cortex in Fig. 1c, in the $\Delta BOLD_{norm}$ map the activation at the edge of the brain was weak

(Fig. 1d). In both the motor task ΔR_2^* map and the $\Delta BOLD_{norm}$ map, activation within the motor areas was evident, but shifts in the location of the centroids of activation were observed.

In Fig. 2b, ΔR_2^* vs. $\Delta BOLD_{norm}$ for the finger movement task is plotted for all pixels with values greater than zero (open black circles) using the same subject's data as in Fig. 1. The slope of the data is proportional to k_{total} , which is directly related to CBV_v . Samples of these pixels were chosen by specifying an ROI around the superior sagittal sinus and an ROI in the sensorimotor area (Fig. 1). As shown (Fig. 2b), pixels from the superior sagittal sinus area (filled blue circles) fall along a trajectory of low $\Delta BOLD_{norm}$ (i.e., low oxygenation changes) and can reach high values of ΔR_2^* . In contrast, pixels chosen from within the sensorimotor cortex (filled red circles), where high functional activity is expected, are distributed along an axis that is relatively low in ΔR_2^* compared to the sinus region but reaches higher values of $\Delta BOLD_{norm}$. The extremes of these trajectories represent two distinct classes of voxels: those containing large vessels distant from the site of activation (i.e., high ΔR_2^* , low $\Delta BOLD_{norm}$) and those containing small vessels within the active site (i.e., low ΔR_2^* , high $\Delta BOLD_{norm}$). These observations are consistent with the findings of Bandettini and Wong (1997). Most active voxels fall in between these two axes and likely represent voxels with a mixture of large and small vessels or voxels that contain large vessels that are near

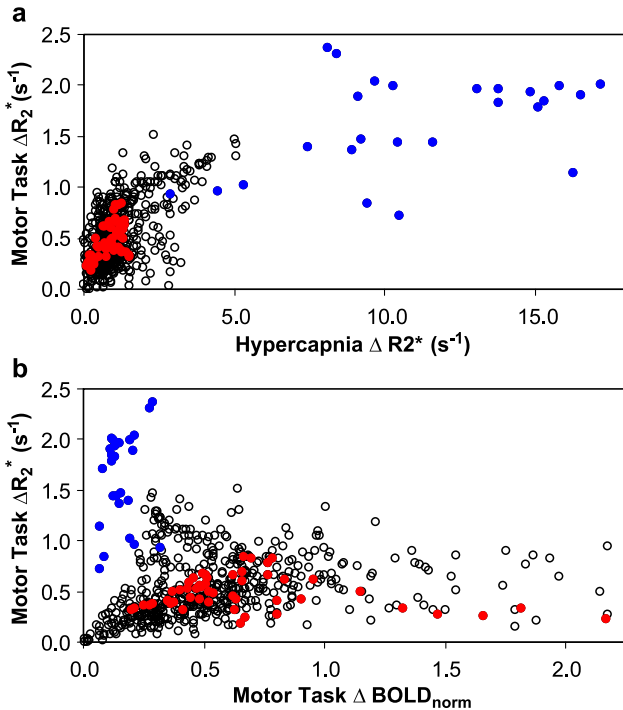


Fig. 2. (a) A plot of ΔR_2^* from all pixels (open black circles) active during the motor task vs. their values during hypercapnia from the same subject scanned at 4 T as in Fig. 1. (b) A plot of ΔR_2^* from all pixels (open black circles) active during the motor task vs. their normalized BOLD values from the same subject. The red-filled circles correspond to those pixels within the small motor cortex ROI in Fig. 1. The blue-filled circles represent a sample of pixels from large vessels, corresponding to those pixels within the superior sagittal sinus ROI in Fig. 1. The shallower slope of the large vessel pixels compared to the small vessel pixels is apparent (a), indicating that the large vessel areas distant from the activation site undergo less of an oxygenation change during neural stimulation than the truly active regions. Voxels in which the blood volume fraction is dominated by large vessels tend to have relatively higher values of ΔR_2^* and low normalized BOLD responses. The color coding of the pixels follows the same convention in b so that the effect of normalization on these two distinct groups of pixels can be appreciated.

the sites of activation and therefore undergo moderate to large changes in blood oxygenation.

The sensitivity of the BOLD signal is strongly dependent on magnetic field strength (Ogawa et al., 1998). At higher magnetic field, the relative sensitivity to tissue increases while the sensitivity to large draining veins decreases (Gati et al., 1997; Ogawa et al.,

1998; Yacoub et al., 2001). An example of results obtained at 7 T is shown in Fig. 3. Differences between the ΔR_2^* and $\Delta BOLD_{\text{norm}}$ hot spots may be less apparent at 7 T than at lower magnetic fields due to the preferential enhancement of small vessels over large vessels at very high magnetic fields.

Quantitative normalization of BOLD signal changes

Both hypercapnia-induced and motor task-related GE ΔR_2^* increase roughly linearly with B_0 , which can be seen for active pixels within the motor region ROI during hypercapnia and during motor activation (Fig. 4 and Table 1). A one-way analysis of variance (ANOVA) was used to test for significant differences between the mean hypercapnia-induced ΔR_2^* obtained with the GE sequence at each B_0 . One-way ANOVA (i.e., t test) was also performed to test for differences between the mean 4-T GE ΔR_2^* and SE ΔR_2 values. The same statistical comparisons were made for the motor-induced quantities. Significant differences in both hypercapnia-induced GE ΔR_2^* and motor task-related GE ΔR_2^* were found ($P < 0.01$ with $F = 7.16$, $df_1 = 2$, $df_2 = 13$ and $P < 0.001$ with $F = 14.49$, $df_1 = 2$, $df_2 = 13$, respectively). Significant differences were also found between 4-T GE ΔR_2^* and SE ΔR_2 induced by hypercapnia ($P < 0.01$, one-tailed, unpaired, unequal variance) and between those induced by the motor task ($P < 0.005$, one-tailed, unpaired, unequal variance). As expected, ΔR_2 obtained with the SE sequence is approximately 3–4 times less than ΔR_2^* obtained with the GE sequence at 4 T. The dependence of the BOLD signal on field strength and pulse sequences, demonstrated in this study and elsewhere (Gati et al., 1997), hampers comparison of data obtained with different experimental parameters and from different laboratories.

Hypercapnic normalization was used to quantitatively compare the results of the motor task. The average motor task-related ΔR_2^* (or SE ΔR_2) of active pixels within each subject's motor region ROI (Fig. 3) was divided by the average hypercapnia-induced ΔR_2^* (or SE ΔR_2) of the same pixels to yield an average $\Delta BOLD_{\text{norm}}$ for the active region (Fig. 4 and Table 1). The average rCBF within this ROI (Fig. 3) was also calculated for each subject (Fig. 4 and Table 1). Intersubject mean $\Delta BOLD_{\text{norm}}$ values were calculated for each field strength and pulse sequence (Table 1). A one-way ANOVA was performed to test for differences between the mean $\Delta BOLD_{\text{norm}}$ values obtained with the GE sequence at each B_0 . A t test was performed to test for differences between the mean $\Delta BOLD_{\text{norm}}$ values of the GE and SE 4-T data. No significant differences between group means were found with these tests, suggesting that the normalization procedure works

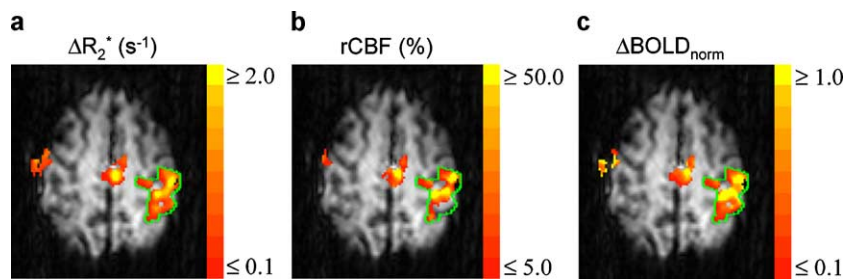


Fig. 3. Data from one subject at 7 T showing the motor region ROI (green line) used in calculating the mean regional values for this subject. The ΔR_2^* (a), rCBF (b), and $\Delta BOLD_{\text{norm}}$ (c) maps are shown overlaid on the average non-slice-selective inversion recovery image for comparison of activation hot spots (yellow pixels). The ROI was drawn based on the ΔR_2^* map to include activation within the motor and somatosensory areas on the contralateral side of the finger movement.

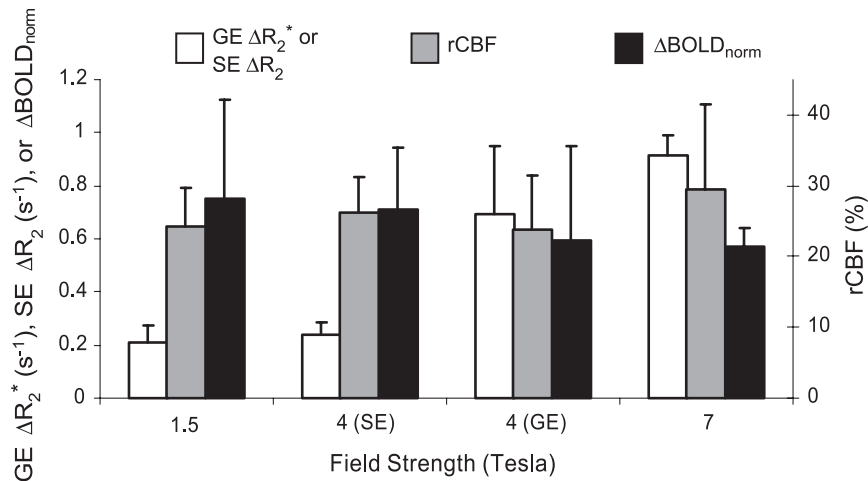


Fig. 4. A comparison of ΔR_2^* , ΔR_2 , rCBF, and $\Delta BOLD_{norm}$ averaged over all subjects at each magnetic field strength ($n = 5$, $n = 8$, and $n = 3$ for the GE studies at 1.5, 4, and 7 T, respectively and $n = 6$ for the SE study at 4 T). Error bars represent one standard deviation. The mean rCBF did not significantly differ across field strength nor did the mean $\Delta BOLD_{norm}$. No significant differences were found between the mean GE and SE rCBF and $\Delta BOLD_{norm}$ values, as described in detail in the text and Table 1.

similarly at all field strengths employed in this study. The field-independent nature of the normalized BOLD signal within the motor region ROI is similar to that of the rCBF signal within the same region (Fig. 4 and Table 1).

Discussion

The ratio $\Delta BOLD_{norm}$ is an index of change in blood oxygenation relative to the hypercapnic control task and, unlike the BOLD signal change itself, is less dependent on resting CBV_v . Therefore, like relative changes in perfusion, it is more closely related to changes in metabolic activity, both spatially and quantitatively. Spatially, this was demonstrated by comparing the locations of high activity in the ΔR_2^* or ΔR_2 motor activation map with those of the $\Delta BOLD_{norm}$ map (Fig. 1). In the ΔR_2^* and ΔR_2 maps, clusters of high activity could be seen within the gray matter in expected locales of functional activation and, in distinct contrast, within the superior sagittal sinus. The sagittal sinus showed relatively weak activation in the normalized map, clearly demonstrating the effectiveness of the technique. However, there were also discrete clusters of activity on the medial and lateral edges of the brain, which are drained by the superior cerebral veins. In such regions, the normalization procedure is most needed. While superior sagittal sinus activation can be easily identified and removed based on its anatomical location, this cannot be done for activation-induced changes in areas in which it is not clear whether the activation is actually due to large vessels in the region or due to large task-specific oxygenation changes. One such ambiguous area in the interhemispheric fissure is indicated by a green arrow in Fig. 1c. This territory may be activated because of the presence of large veins or because of high activity in the motor areas of the medial walls of the cortex. Due to this uncertainty in the source of strong BOLD signal changes, such activation foci are typically included without qualification in the final activation map despite their potential for providing misleading activity localization and magnitude information.

In pixels with a presumed mixture of large and small vessels or large vessels that are near the sites of activation and therefore

undergo significant changes in blood oxygenation, the normalization procedure has apparently minimized the dependence of BOLD signals on resting CBV_v . Note that normalization has not removed the dependence on baseline CBV_v and hence large vessels still make some contribution to the final signal. However, the bias toward large veins inherent in the conventional BOLD signal has been substantially reduced. It is possible that SE as opposed to GE imaging (Boxerman et al., 1995b; Kennan et al., 1994; Lee et al., 1999; Ogawa et al., 1993; Yacoub et al., 2003) in combination with hypercapnic normalization could provide an additional advantage in macrovascular signal reduction and improved spatial localization of activity. The SE and GE data were not collected in the same subjects in this study and therefore an accurate appraisal of such a strategy is not feasible from our data. The large-vessel contribution may also be further minimized by utilizing diffusion weighting gradients (Boxerman et al., 1995a; Lee et al., 1999; Song et al., 1996) in conjunction with hypercapnic normalization. Evaluation of these combined methodologies is certainly warranted and encouraged by our results and those of Bandettini and Wong (1997).

Knowing that the $\Delta BOLD_{norm}$ map is not weighted by resting CBV_v and that it is proportional to changes in oxygenation, we can assume that the $\Delta BOLD_{norm}$ map is a more spatially precise, albeit indirect, marker of brain activity. Note that, in principle, large changes in oxygenation can occur in large veins simply due to their proximity to sites of high neuronal activity. This implies that these proximal large veins would have high $\Delta BOLD_{norm}$ values. As oxygenated hemoglobin flows distally from activation sites, it should become diluted by the deoxygenated hemoglobin content of veins draining nearby inactive or less active regions of cortex (Turner, 2002). Such distal veins will constitute voxels with low values of $\Delta BOLD_{norm}$. The caveat of large-vessel activation in the typical BOLD map is that the signal magnitude is essentially proportional to vessel size despite a low activity-specific, oxygenation change. This consideration is alleviated when examining the $\Delta BOLD_{norm}$ map because the resting CBV_v weighting inherent in ΔR_2^* or ΔR_2 is diminished; changes in $\Delta BOLD_{norm}$ are then indeed commensurate with changes in functional activity, whether the signal originates from capillaries

at the active site or slightly larger vessels that are very close to the active site.

The $\Delta\text{BOLD}_{\text{norm}}$ magnitude can also be used to provide a quantitative estimate of the level of activity involved in a particular task that can be compared to other normalized results without regard to differences in field strength or pulse sequence. This was demonstrated in the comparison of the average $\Delta\text{BOLD}_{\text{norm}}$ values in Table 1 and their relationship to changes in CBF. On average, the magnitude of $\Delta\text{BOLD}_{\text{norm}}$ is the same across subjects and B_0 for the task employed in this study. It is also the same regardless of whether a GE or SE sequence is used at 4 T. To corroborate the fact that the motor task did cause the same average level of activation in all subject groups, the average rCBF level was computed from the FAIR data and was found not to differ across groups (Table 1).

It is possible to underestimate perfusion when volume or head coils, rather than whole body coils, are used for transmission of the inversion pulse in pulsed arterial spin labeling experiments. For both radio frequency (RF) transmission and detection, our experiments relied upon head coils that covered the head but not the neck and body. When using head coils for RF transmission, uninverted spins outside of the field of view of the coil may travel into the imaging slice during acquisition of the FAIR control images, reducing the sensitivity of perfusion contrast. Although this situation is likely to be more problematic when global CBF changes are induced, it is possible that it caused an error in determining the focal relative CBF changes in our motor task data. However, based on our previous comparison studies of CBF changes measured by FAIR and H_2^{15}O PET in the same subjects, we found that relative CBF changes in the motor regions induced by finger movements were consistent (Zaini et al., 1999). CBF changes measured by FAIR during self-paced bilateral finger tapping and visual stimulation have also been corroborated by a bolus tracking technique in individual subjects (Li et al., 2000). Furthermore, our motor task-induced CBF changes at three magnetic field strengths agree well. Therefore, such concerns do not seem germane to our results.

One of the concerns with the hypercapnic normalization method relates to the potential for causing sensory stimulation and therefore brain activation due to air hunger (Banzett et al., 2000; Brannan et al., 2001; Corfield et al., 1995; Evans et al., 2002; Liotti et al., 2001; Parsons et al., 2001). Other expressions that are related to “air hunger” include “dyspnea” (i.e., uncomfortable or difficult breathing), “breathlessness”, “shortness of breath”, “urge to breathe”, and “increased work/effort of breathing”. The difference between such expressions is not merely semantic but perceptual (Moosavi et al., 2003; Simon et al., 1989) and can be experimentally dissociated by employing different respiratory stimuli (Lansing et al., 2000). Spontaneous breathing of CO_2 gas mixtures, when distinguishable from breathing normal air, tends to be associated with sensations of an urge to breathe, rapid breathing, and increased respiratory work (Moosavi et al., 2003; Simon et al., 1989), especially at high ETCO_2 . When given a choice of descriptors for their sensations, the term “air hunger” was also sometimes chosen by Moosavi et al.’s subjects at a mean ETCO_2 of approximately 46 mm Hg. However, the same subjects at the same ETCO_2 level rarely chose the descriptors “starved for air” or “short of breath” (Moosavi et al., 2003). Similarly, Banzett et al. (1996) and Shea et al. (1996) reported minimal if any sensations of air hunger at a mean ETCO_2 of approximately 46 mm Hg during spontaneous breathing of CO_2 gas. In Shea et al.’s study, moderate air hunger was not evoked until the mean ETCO_2 was greater than

52 mm Hg. Therefore, at ETCO_2 levels and under experimental conditions comparable to those used in our experiments, the hypercapnia experience has methodically been shown to be infrequently associated with uncomfortable sensations of air hunger.

Although we did not systematically collect psychophysical data in relation to hypercapnia, our experience has also shown that the relatively low degree of hypercapnia involved in our studies tends not to cause uncomfortable breathing sensations. Subjects in the present study had no difficulties undergoing hypercapnia and no complaints of discomfort. Of note, using the identical protocol as in the current investigation, subjects in our previous study (Cohen et al., 2002) underwent several consecutive repetitions of the 5% CO_2 inhalation experiment during individual sessions without difficulty or complaints of dyspnea. Hoge et al. (1999), who used inhalation of CO_2 at various concentrations to calibrate the BOLD response, also stated that their subjects did not experience untoward effects, even at the highest level of 5% CO_2 . Therefore, hypercapnia induced by 5% CO_2 inhalation resulting in ETCO_2 levels of 46–48 mm Hg seems to be below the threshold of air hunger for most subjects and its use for hypercapnic normalization does not appear problematic. Nevertheless, to more thoroughly avoid the possibility of neural activation secondary to hypercapnia, lower concentrations of inspired CO_2 such as 3% or 4% could be used instead of 5% CO_2 for the purpose of normalization. A target ETCO_2 level of approximately 44 mm Hg, which is well below the level of detectability (e.g., see Banzett et al., 2000), may be a more conservative goal. Minimizing the duration of hypercapnia may also help to reduce detection of CO_2 -induced physiological changes, as suggested by the results of Maresh et al. (1997), because changes in ventilation and peak air hunger ratings slightly lag behind the ETCO_2 changes (see, for example, Fig. 2 and text in Adams et al., 1985 and Fig. 2 in Shea et al., 1996). Ultimately, it is the increase in arterial partial pressure of carbon dioxide (P_{CO_2}) that drives the changes in CBF, however, and sufficient time must be allowed for this response to evolve.

Although functional imaging studies have reported activation in limbic and paralimbic structures, the cerebellum, and other areas during air hunger (Banzett et al., 2000; Brannan et al., 2001; Corfield et al., 1995; Evans et al., 2002; Gozal et al., 1994; Parsons et al., 2001; Peiffer et al., 2001; Liotti et al., 2001), these results must be interpreted judiciously, with particular attention to the functional imaging modality, the methods used to induce air hunger, the subjective sensory experiences of the subjects, and the investigators’ choice of control conditions. It is also important to realize that these experiments were deliberately designed to induce moderate or severe air hunger. To this end, with the exception of Corfield et al. (1995), whose subjects breathed a 5% CO_2 gas mixture, potent dyspnea-inducing stimuli were used. Therefore, evaluating the use of mild hypercapnia as a global vasodilator independent of neural activation is difficult based on their results.

For instance, Evans et al.’s (2002) and Banzett et al.’s (2000) functional imaging studies involved passive mechanical ventilation. Air hunger was induced by maintaining the tidal volume (V_T) at constant reduced amplitude and the ETCO_2 at a fixed elevated level. Our study involved free breathing during normocapnia and during hypercapnia, which was induced by CO_2 inhalation only. Specifically, two or three 2-l reservoir bags and adequate air flow, which was titrated for each subject, ensured that sufficient volume was available and that breathing was unrestricted. This methodological distinction is important for two reasons. First, restricting

ventilation itself leads to a sensation of breathlessness or air hunger that may be qualitatively different from sensations such as the urge to breathe and increased respiratory effort (Banzett et al., 1996; Lansing et al., 2000) more commonly associated with high levels of ETCO_2 during spontaneous ventilation (Moosavi et al., 2003; Simon et al., 1989). In fact, the combination of hypercapnia and restricted V_T actually exacerbates air hunger (e.g., Manning et al., 1992), extreme sensations of which can be almost completely relieved by increased spontaneous ventilation at elevated inspired PCO_2 (Banzett et al., 1996, 2000; Bloch-Salisbury et al., 1998; Shea et al., 1996). Put another way, the threshold for detection of air hunger under hypercapnic free-breathing conditions is higher than it is for hypercapnia in conjunction with reduced V_T . This physiological phenomenon is what enabled Banzett et al. (2000) to use free breathing at an elevated ETCO_2 of 44 mm Hg as their control condition for air hunger induced by restricted V_T at the same elevated ETCO_2 . Therefore, at least some of the perceptions of air hunger evoked and measured by Banzett et al. (2000) and Evans et al. (2002) may be different from those evoked by spontaneously breathing high levels of CO_2 (e.g., compare the frequency of subjects' responses in Fig. 3 of Evans et al., 2002 with those of Simon et al., 1989 and Moosavi et al., 2003). The second point is that both groups of investigators noted that suppression of motor activity in response to the urge to override the ventilator may have accounted for the activity seen in the supplementary motor areas and frontal premotor areas. Because breathing was unrestricted in our study, activation of structures due to suppression of the urge to breathe was unlikely. Additionally, no primary motor cortical activity was seen in Evans et al.'s or Banzett et al.'s studies. Therefore, in terms of being applicable to studies of premotor, supplementary motor, and primary sensorimotor cortex, the hypercapnic normalization method appears generally valid. A similar argument to that above may be made regarding the interpretation of Peiffer et al.'s (2001) PET results of air hunger induced by breathing against resistive loads.

Corfield et al. (1995) also observed cortical activation in limbic structures under hypercapnic spontaneous breathing conditions compared with normocapnic passive mechanical ventilation. However, the mean hypercapnic ETCO_2 of Corfield et al.'s subjects (50.3 mm Hg) was slightly higher than that of our subjects in both the present study and our previous one (Cohen et al., 2002), a difference that could be significant perceptually. Corfield et al.'s and Gozal et al.'s (1994) studies also underscore the difficulty and importance of devising a satisfactory control condition for functional imaging studies of air hunger. For instance, isocapnic mechanical ventilation, which served as the control condition in Corfield et al.'s study, evokes its own sensations, descriptions of which Corfield et al. provided from a separate group of study participants, and therefore may have been inadequate as a behavioral control. An equally important consideration is that induction of air hunger involves manipulation of blood gases (i.e., O_2 and CO_2), which have direct hemodynamic effects in the central nervous system. Experimentally controlling for regional differences due to the direct hemodynamic influence of CO_2 (Ito et al., 2000) is challenging and may not have been achieved by Corfield et al. or by Gozal et al. (1994), who used a similar study design. In this regard, Banzett et al.'s (2000) use of an ETCO_2 of 44 mm Hg as a control condition for their BOLD fMRI measurements of air hunger was an excellent choice, especially in light of the BOLD response's proportionality to baseline CBV_v . However, hemodynamic responses to the sensations of air hunger,

which are the quantities of interest in all of these studies, are evoked on top of the altered hemodynamic baseline. Human functional imaging studies have demonstrated that the hemodynamic response to neural stimulation is influenced by the baseline level of CBF when modulated by hypercapnia or hyperventilation (Bandettini and Wong, 1997; Cohen et al., 2002; Kemna et al., 2001; Posse et al., 2001; Shimosegawa et al., 1995) and hyperoxia or hypoxia (Bandettini and Wong, 1997; Kashikura et al., 2000, 2001). This effect was mentioned by Evan's et al. (2002) as a possible confound. Functional imaging studies of air hunger may have to additionally control for the interaction between the global effects of arterial PO_2 and PCO_2 and the focal hemodynamic response.

Other functional imaging studies had subjects spontaneously breathe hyperoxic gas mixtures consisting of moderately high levels of CO_2 (i.e., 8% CO_2 , 92% O_2) to evoke uncomfortable sensations of air hunger (Brannan et al., 2001; Liotti et al., 2001; Parsons et al., 2001). At this level of hypercapnia, perceptions of air hunger during spontaneous breathing would be expected to far exceed any potentially evoked ETCO_2 levels comparable to ours (46–48 mm Hg), which are minimal if noticeable at all (Banzett et al., 1996; Cohen et al., 2002; Moosavi et al., 2003). Interestingly, Liotti et al. (2001) found that subjective ratings of air hunger were significantly lower when subjects breathed the CO_2 gas mixture through a mouthpiece (as in our study) rather than a face mask, despite the mean ETCO_2 level being equivalent in both conditions.

Given the experimental conditions we created of unrestricted ventilation and relatively low inspired concentrations of CO_2 , as well as our subjects' apparent lack of difficulty undergoing hypercapnia, the perception of air hunger and associated neural activation do not seem to be a great concern in our study. Although further studies would be necessary to systematically investigate the potential activation induced by 5% CO_2 gas inhalation in our experimental protocol, hypercapnic normalization seems to be a widely applicable method that improves the spatial specificity of BOLD signals in cortical regions. Furthermore, our theoretical description and empirical observations of the effect of hypercapnic normalization support the idea that the measured changes in $\Delta\text{BOLD}_{\text{norm}}$ are proportional to oxygenation changes and are independent of other factors, because a given task should produce similar changes in oxygenation level irrespective of the measurement parameters. This property of the normalized BOLD signal can be used to quantitatively compare the level of activity of a given task across experimental conditions such as field strength and pulse sequence, and can also be used to quantitate activity with respect to various parameters of the task itself.

The benefit of the normalization procedure for mapping active tissue is that it uses the BOLD signal only, which does not suffer from the signal-to-noise limitations that, for example, CBF-based methods do. It also normalizes both intravascular and extravascular large venous signals, in contrast to SE and diffusion-weighted methods alone. These properties allow for more accurate pixel-by-pixel analysis and can be adapted for high spatial resolution studies. For example, ocular dominance columns and other types of cortical columns might potentially be resolved by normalizing for the non-column-specific CBV_v response with a hypercapnia percent change map. Keeping the voxel size small would minimize the partial volume effect of large vessels and small vessels mixing within voxels, and enhance the distinction of such voxels. Hypercapnic normalization may also hold promise in neurosurgical preoperative planning in which large veins impede the accurate spatial local-

ization necessary for making informed therapeutic decisions (Krings et al., 2001). The hypercapnic normalization procedure has also been demonstrated to provide quantitatively consistent results across experimental conditions, namely field strength and pulse sequence. Therefore, it can be used as a means of quantitatively evaluating task activation. Relative contributions to task-related activity from various brain regions may be accurately inferred from normalized fMRI data and compared with such data acquired using different MRI systems and pulse sequences.

Acknowledgments

Supported by the National Institutes of Health (EB00201, EB00337, EB00332, EB00331, and RR08079), the Keck Foundation and the MIND Institute.

References

- Adams, L., Chronos, N., Lane, R., Guz, A., 1985. The measurement of breathlessness induced in normal subjects: validity of two scaling techniques. *Clin. Sci.* 69, 7–16.
- Bandettini, P.A., Wong, E.C., 1997. A hypercapnia-based normalization method for improved spatial localization of human brain activation with fMRI. *NMR Biomed.* 10, 197–203.
- Bandettini, P.A., Wong, E.C., Jesmanowicz, A., Hinks, R.S., Hyde, J.S., 1994. Spin-echo and gradient-echo EPI of human brain activation using BOLD contrast: a comparative study at 1.5 T. *NMR Biomed.* 7, 12–20.
- Banzett, R.B., Lansing, R.W., Evans, K.C., Shea, S.A., 1996. Stimulus-response characteristics of CO₂-induced air hunger in normal subjects. *Respir. Physiol.* 103, 19–31.
- Banzett, R.B., Mulnier, H.E., Murphy, K., Rosen, S.D., Wise, R.J.S., Adams, L., 2000. Breathlessness in humans activates insular cortex. *NeuroReport* 11, 2117–2120.
- Bloch-Salisbury, K., Spengler, C.M., Brown, R., Banzett, R.B., 1998. Self-control and external control of mechanical ventilation give equal air hunger relief. *Am. J. Respir. Crit. Care Med.* 157, 415–420.
- Boxerman, J.L., Bandettini, P.A., Kwong, K.K., Baker, J.R., Davis, T.L., Rosen, B.R., Weisskoff, R.M., 1995a. The intravascular contribution to fMRI signal change: Monte Carlo modeling and diffusion-weighted studies in vivo. *Magn. Reson. Med.* 34, 4–10.
- Boxerman, J.L., Hamberg, L.M., Rosen, B.R., Weisskoff, R.M., 1995b. MR contrast due to intravascular magnetic susceptibility perturbations. *Magn. Reson. Med.* 34, 555–566.
- Brannan, S., Liotti, M., Egan, G., Shade, R., Madden, L., Robillard, R., Abplanalp, B., Stofer, K., Denton, D., Fox, P.T., 2001. Neuroimaging of cerebral activations and deactivations associated with hypercapnia and hunger for air. *Proc. Natl. Acad. Sci. U. S. A.* 98, 2029–2034.
- Carpenter, M.B., 1991. *Core Text of Neuroanatomy*, fourth ed. Williams and Wilkins, Philadelphia.
- Cohen, E.R., Ugurbil, K., Kim, S.-G., 2002. Effect of basal conditions on the magnitude and dynamics of the blood oxygenation level-dependent fMRI response. *J. Cereb. Blood Flow Metab.* 22, 1042–1053.
- Corfield, D.R., Fink, G.R., Ramsay, S.C., Murphy, K., Harty, H.R., Watson, J.D.G., Adams, L., Frackowiak, R.S.J., Guz, A., 1995. Evidence for limbic system activation during CO₂-stimulated breathing in man. *J. Physiol.* 488, 77–84.
- Davis, T.L., Kwong, K.K., Weisskoff, R.M., Rosen, B.R., 1998. Calibrated functional MRI: mapping the dynamics of oxidative metabolism. *Proc. Natl. Acad. Sci. U. S. A.* 95, 1834–1839.
- Duong, T.Q., Yacoub, E., Adriany, G., Hu, X., Ugurbil, K., Kim, S.-G., 2003. Microvascular BOLD contribution at 4 and 7 T in the human brain: gradient-echo and spin-echo fMRI with suppression of blood effects. *Magn. Reson. Med.* 49, 1010–1027.
- Edelman, R.R., Siewert, B., Darby, D.G., Thangaraj, V., Nobre, A.C., Mesulam, M.M., Warach, S., 1994. Qualitative mapping of cerebral blood flow and functional localization with echo-planar MR imaging and signal targeting with alternating radio frequency. *Radiology* 192, 513–520.
- Evans, K.C., Banzett, R.B., Adams, L., McKay, L., Frackowiak, R.S.J., Corfield, D.R., 2002. BOLD fMRI identifies limbic, paralimbic, and cerebellar activation during air hunger. *J. Neurophysiol.* 88, 1500–1511.
- Frahm, J., Merboldt, K.-D., Hänicke, W., Kleinschmidt, A., Boecker, H., 1994. Brain or vein-oxygenation or flow? On signal physiology in functional MRI of human brain activation. *NMR Biomed.* 7, 45–53.
- Friston, K.J., Ashburner, J., Poline, J.B., Frith, C.D., Heather, J.D., Frackowiak, R.S.J., 1995. Spatial registration and normalisation of images. *Hum. Brain Mapp.* 2, 165–189.
- Gati, J.S., Menon, R.S., Ugurbil, K., Rutt, B.K., 1997. Experimental determination of the BOLD field strength dependence in vessels in tissue. *Magn. Reson. Med.* 38, 296–302.
- Gozal, D., Hathout, G.M., Kirlew, K.A.T., Tang, H., Woo, M.S., Zhang, J., Lufkin, R.B., Harper, R.M., 1994. Localization of putative neural respiratory regions in the human by functional magnetic resonance imaging. *J. Appl. Physiol.* 76, 2076–2083.
- Grubb, R.L., Raichle, M.E., Eichling, J.O., Ter-Pogossian, M.M., 1974. The effect of changes in PaCO₂ on cerebral blood flow, blood volume, and vascular mean transit time. *Stroke* 5, 630–639.
- Haacke, E.M., Lai, S., Reichenback, J.R., Kuppusamy, K., Hoogenraad, F.G.C., Takeichi, H., Lin, W., 1997. In vivo measurement of blood oxygen saturation using magnetic resonance imaging: a direct validation of the blood oxygen level-dependent concept in functional brain imaging. *Hum. Brain Mapp.* 5, 341–346.
- Hoge, R.D., Atkinson, J., Gill, B., Crelier, G.R., Marrett, S., Pike, G.B., 1999. Investigation of BOLD signal dependence on cerebral blood flow and oxygen consumption: the deoxyhemoglobin dilution model. *Magn. Reson. Med.* 42, 849–863.
- Hyder, F., Kida, I., Behar, K.L., Kennan, R.P., Maciejewski, P.K., Rothman, D.L., 2001. Quantitative functional imaging of the brain: towards mapping neuronal activity by BOLD fMRI. *NMR Biomed.* 14, 413–431.
- Ito, H., Yokoyama, I., Iida, H., Kinoshita, T., Hatazawa, J., Shimosegawa, E., Okudera, T., Kanno, I., 2000. Regional differences in cerebral vascular response to P_aCO₂ changes in humans measured by positron emission tomography. *J. Cereb. Blood Flow Metab.* 20, 1264–1270.
- Kashikura, K., Kershaw, J., Kashikura, A., Matsuura, T., Kanno, I., 2000. Hyperoxia-enhanced activation-induced hemodynamic response in human VI: an fMRI study. *NeuroReport* 11, 903–906.
- Kashikura, K., Kershaw, J., Kashikura, A., Zhang, X., Matsuura, T., Kanno, I., 2001. Hyperoxia modified activation-induced blood oxygenation level-dependent response of human visual cortex (V1): an event-related functional magnetic resonance imaging study. *Neurosci. Lett.* 299, 53–56.
- Kastrup, A., Krügger, G., Neumann-Haefelin, T., Moseley, M.E., 2001. Assessment of cerebrovascular reactivity with functional magnetic resonance imaging: comparison of CO₂ and breath holding. *Magn. Reson. Imaging* 19, 13–20.
- Kemna, L.J., Posse, S., Tellmann, L., Schmitz, T., Herzog, H., 2001. Interdependence of regional and global cerebral blood flow during visual stimulation: an O-15-butanol positron emission tomography study. *J. Cereb. Blood Flow Metab.* 21, 664–670.
- Kennan, R.P., Zhong, J., Gore, J.C., 1994. Intravascular susceptibility contrast mechanisms in tissues. *Magn. Reson. Med.* 31, 9–21.
- Kety, S.S., Schmidt, C.F., 1948. The effects of altered arterial tensions of carbon dioxide and oxygen on cerebral blood flow and cerebral oxygen consumption of normal young men. *J. Clin. Invest.* 27, 484–492.
- Kim, S.-G., 1995. Quantification of relative cerebral blood flow change by flow-sensitive alternating inversion recovery (FAIR) technique: application to functional mapping. *Magn. Reson. Med.* 34, 293–301.

- Kim, S.-G., Tsekos, N.V., 1997. Perfusion imaging by a flow-sensitive alternating inversion recovery (FAIR) technique: application to functional brain imaging. *Magn. Reson. Med.* 37, 425–435.
- Kim, S.-G., Ugurbil, K., 1997. Comparison of blood oxygenation and cerebral blood flow effects in fMRI: estimation of relative oxygen consumption change. *Magn. Reson. Med.* 38, 59–65.
- Kim, S.-G., Rostrup, E., Larsson, H.B.W., Ogawa, S., Paulson, O.B., 1999. Determination of relative CMRO₂ from CBF and BOLD changes: significant increase of oxygen consumption rate during visual stimulation. *Magn. Reson. Med.* 41, 1152–1161.
- Krings, T., Reinges, M.H.T., Erberich, S., Kemeny, S., Rohde, V., Spetzger, U., Korinth, M., Willmes, K., Gilsbach, J.M., Thron, A., 2001. Functional MRI for presurgical planning: problems, artefacts, and solution strategies. *J. Neurol., Neurosurg. Psychiatry* 70, 749–760.
- Kwong, K.K., Belliveau, J.W., Chesler, D.A., Goldberg, I.E., Weisskoff, R.M., Poncelet, B.P., Kennedy, D.N., Hoppel, B.E., Cohen, M.S., Turner, R., Cheng, H.-M., Brady, T.J., Rosen, B.R., 1992. Dynamic magnetic resonance imaging of human brain activity during primary sensory stimulation. *Proc. Natl. Acad. Sci. U. S. A.* 89, 5675–5679.
- Lansing, R.W., Im, B.S.-H., Thwing, J.I., Legedza, A.T.R., Banzett, R.B., 2000. The perception of respiratory work and effort can be independent of the perception of air hunger. *Am. J. Respir. Crit. Care Med.* 162, 1690–1696.
- Lee, S.-P., Silva, A.C., Ugurbil, K., Kim, S.-G., 1999. Diffusion-weighted spin-echo fMRI at 9.4 T: microvascular/tissue contribution to BOLD signal change. *Magn. Reson. Med.* 42, 919–928.
- Lee, S.-P., Duong, T.Q., Yang, G., Iadecola, C., Kim, S.-G., 2001. Relative changes of cerebral arterial and venous blood volumes during increased cerebral blood flow: implications for BOLD fMRI. *Magn. Reson. Med.* 45, 791–800.
- Li, T.-Q., Haefelin, T.N., Chan, B., Kastrup, A., Jonsson, T., Glover, G.H., Moseley, M.E., 2000. Assessment of hemodynamic response during focal neural activity in human using bolus tracking, arterial spin labeling and BOLD techniques. *NeuroImage* 12, 442–451.
- Liotti, M., Brannan, S., Egan, G., Shade, R., Madden, L., Abplanalp, B., Robillard, R., Lancaster, J., Zamarripa, F.E., Fox, P.T., Denton, D., 2001. Brain responses associated with consciousness of breathlessness (air hunger). *Proc. Natl. Acad. Sci. U. S. A.* 98, 2035–2040.
- Manning, H.L., Shea, S.A., Schwartzstein, R.M., Lansing, R.W., Brown, R., Banzett, R.B., 1992. Reduced tidal volume increases 'air hunger' at fixed PCO₂ in ventilated quadriplegics. *Respir. Physiol.* 90, 19–30.
- Maresh, C.M., Armstrong, L.E., Kavouras, S.A., Allen, G.J., Casa, D.J., Whittlesey, M., LaGasse, K.E., 1997. Physiological and psychological effects associated with high carbon dioxide levels in healthy men. *Aviat., Space Environ. Med.* 68, 41–45.
- Menon, R.S., Ogawa, S., Tank, D.W., Ugurbil, K., 1993. 4 Tesla gradient recalled echo characteristics of photic stimulation-induced signal changes in the human primary visual cortex. *Magn. Reson. Med.* 30, 380–386.
- Moosavi, S.H., Golestanian, E., Binks, A.P., Lansing, R.W., Brown, R., Banzett, R.B., 2003. Hypoxic and hypercapnic drives to breathe generate equivalent levels of air hunger in humans. *J. Appl. Physiol.* 94, 141–154.
- Ngai, A.C., Meno, J.R., Winn, H.R., 1995. Simultaneous measurements of pial arteriolar diameter and laser-Doppler flow during somatosensory stimulation. *J. Cereb. Blood Flow Metab.* 15, 124–127.
- Ogawa, S., Menon, R.S., Tank, D.W., Kim, S.-G., Merkle, H., Ellermann, J.M., Ugurbil, K., 1993. Functional brain mapping by blood oxygenation level-dependent contrast magnetic resonance imaging: a comparison of signal characteristics with a biophysical model. *Biophys. J.* 64, 803–812.
- Ogawa, S., Menon, R.S., Kim, S.-G., Ugurbil, K., 1998. On the characteristics of functional magnetic resonance imaging of the brain. *Annu. Rev. Biophys. Biomol. Struct.* 27, 447–474.
- Oja, J.M.E., Gillen, J., Kauppinen, R.A., Kraut, M., van Zijl, P.C.M., 1999. Venous blood effects in spin-echo fMRI of human brain. *Magn. Reson. Med.* 42, 617–626.
- Osborn, A.G., 1994. *Diagnostic Neuroradiology*. Mosby, St. Louis.
- Parsons, L.M., Egan, G., Liotti, M., Brannan, S., Denton, D., Shade, R., Robillard, R., Madden, L., Abplanalp, B., Fox, P.T., 2001. Neuroimaging evidence implicating cerebellum in the experience of hypercapnia and hunger for air. *Proc. Natl. Acad. Sci. U. S. A.* 98, 2041–2046.
- Peiffer, C., Poline, J.-B., Thivard, L., Aubier, M., Samson, Y., 2001. Neural substrates for the perception of acutely induced dyspnea. *Am. J. Respir. Crit. Care Med.* 163, 951–957.
- Posse, S., Kemna, L.J., Elghahwagi, B., Wiese, S., Kiselev, V.G., 2001. Effect of graded hypo- and hypercapnia on fMRI contrast in visual cortex: quantification of T₂* changes by multiecho EPI. *Magn. Reson. Med.* 46, 264–271.
- Rosen, B.R., Belliveau, J.W., Aronen, H.J., Kennedy, D., Buchbinder, B.R., Fischman, A., Gruber, M., Glas, J., Weisskoff, R.M., Cohen, M.S., Hochberg, F.H., Brady, T.J., 1991. Susceptibility contrast imaging of cerebral blood volume: human experience. *Magn. Reson. Med.* 22, 293–299.
- Rostrup, E., Larsson, H.B.W., Toft, P.B., Garde, K., Thomsen, C., Ring, P., Sondergaard, L., Henriksen, O., 1994. Functional MRI of CO₂ induced increase in cerebral perfusion. *NMR Biomed.* 7, 29–34.
- Rostrup, E., Law, I., Blinkenberg, M., Larsson, H.B.W., Born, A.P., Holm, S., Paulson, O.B., 2000. Regional differences in the CBF and BOLD responses to hypercapnia: a combined PET and fMRI study. *NeuroImage* 11, 87–97.
- Shea, S.A., Harty, H.R., Banzett, R.B., 1996. Self-control of level of mechanical ventilation to minimize CO₂ induced air hunger. *Respir. Physiol.* 103, 113–125.
- Shimosegawa, E., Kanno, I., Hatazawa, J., Fujita, H., Iida, H., Miura, S., Murakami, M., Inugami, A., Ogawa, T., Itoh, H., Okudera, T., Uemura, K., 1995. Photic stimulation study of changing the arterial partial pressure level of carbon dioxide. *J. Cereb. Blood Flow Metab.* 15, 111–114.
- Simon, P.M., Schwartzstein, R.M., Weiss, J.W., Lahive, K., Fencl, V., Teghtsoonian, M., Weinberger, S.E., 1989. Distinguishable sensations of breathlessness induced in normal volunteers. *Am. Rev. Respir. Dis.* 140, 1021–1027.
- Song, A.W., Wong, E.C., Tan, S.G., Hyde, J.S., 1996. Diffusion weighted fMRI at 1.5 T. *Magn. Reson. Med.* 35, 155–158.
- Song, A.W., Woldorff, M.G., Gangstead, S., Mangun, G.R., McCarthy, G., 2002. Enhanced spatial localization of neuronal activation using simultaneous apparent-diffusion-coefficient and blood-oxygenation functional magnetic resonance imaging. *NeuroImage* 17, 742–750.
- Turner, R., 2002. How much cortex can a vein drain? Downstream dilution of activation-related cerebral blood oxygenation changes. *NeuroImage* 16, 1062–1067.
- Vaughan, J.T., Hetherington, H.P., Out, J.O., Pan, J.W., Pohost, G.M., 1994. High frequency volume coils for clinical NMR imaging and spectroscopy. *Magn. Reson. Med.* 32, 206–218.
- Wright, G.A., Hu, B.S., Macovski, A., 1991. Estimating oxygen saturation of blood in vivo with MR imaging at 1.5 T. *J. Magn. Reson. Imaging* 1, 275–283.
- Yacoub, E., Shmuel, A., Pfeuffer, J., Van De Moortele, P.-F., Adriany, G., Andersen, P., Vaughan, J.T., Merkle, H., Ugurbil, K., Hu, K., 2001. Imaging brain function in humans at 7 Tesla. *Magn. Reson. Med.* 45, 588–594.
- Yacoub, E., Duong, T.Q., Van De Moortele, P.-F., Lindquist, M., Adriany, G., Kim, S.-G., Ugurbil, K., Hu, X., 2003. Spin-echo fMRI in humans using high spatial resolutions and high magnetic fields. *Magn. Reson. Med.* 49, 655–664.
- Zaini, M.R., Strother, S.C., Anderson, J.R., Liow, J.S., Kjems, U., Tegeler, C., Kim, S.-G., 1999. Comparison of matched BOLD and FAIR 4.0T-fMRI with ¹⁵O-water PET brain volumes. *Med. Phys.* 26, 1559–1567.